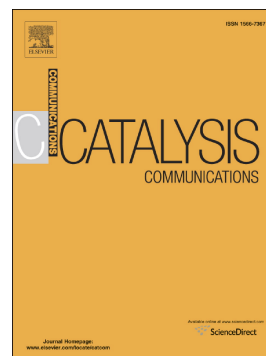


Accepted Manuscript

Simultaneous photocatalytic and catalytic activity of p–n junction NiO@anatase/rutile-TiO₂ as a noble-metal free reusable nanoparticle for synthesis of organic compounds

Abolfazl Ziarati, Alireza Badiei, Ghodsi Mohammadi Ziarani, Hamed Eskandarloo



PII: S1566-7367(17)30074-2
DOI: doi: [10.1016/j.catcom.2017.02.023](https://doi.org/10.1016/j.catcom.2017.02.023)
Reference: CATCOM 4951

To appear in: *Catalysis Communications*

Received date: 26 October 2016
Revised date: 24 January 2017
Accepted date: 23 February 2017

Please cite this article as: Abolfazl Ziarati, Alireza Badiei, Ghodsi Mohammadi Ziarani, Hamed Eskandarloo, Simultaneous photocatalytic and catalytic activity of p–n junction NiO@anatase/rutile-TiO₂ as a noble-metal free reusable nanoparticle for synthesis of organic compounds. The address for the corresponding author was captured as affiliation for all authors. Please check if appropriate. Catcom(2017), doi: [10.1016/j.catcom.2017.02.023](https://doi.org/10.1016/j.catcom.2017.02.023)

This is a PDF file of an unedited manuscript that has been accepted for publication. As a service to our customers we are providing this early version of the manuscript. The manuscript will undergo copyediting, typesetting, and review of the resulting proof before it is published in its final form. Please note that during the production process errors may be discovered which could affect the content, and all legal disclaimers that apply to the journal pertain.

Simultaneous photocatalytic and catalytic activity of p-n junction NiO@anatase/rutile-TiO₂ as a noble-metal free reusable nanoparticle for synthesis of organic compounds

Abolfazl Ziarati^a, Alireza Badiei^{*,a,b}, Ghodsi Mohammadi Ziarani^c, Hamed Eskandarloo^a

^a*School of Chemistry, College of Science, University of Tehran, Tehran, Iran*

^b*Nanobiomedicine Center of Excellence, Nanoscience and Nanotechnology Research Center, University of Tehran, Tehran, Iran*

^c*Department of Chemistry, Faculty of Science, Alzahra University, Tehran, Iran*

Corresponding author. Tel.: +98-21-61112614; Fax: +98-21-61112614

E-mail address: abadiei@khayam.ut.ac.ir (A. Badiei)

Abstract

Photocatalytic and catalytic activity of NiO loaded on mixture of anatase/rutile phases of TiO₂ nanoparticles were investigated for some organic reactions including selective oxidation of alcohols, synthesis of benzimidazoles and preparation of imines at room temperature. The p-n junction formed between NiO and TiO₂ as well as difference between band gaps in anatase/rutile phases facilitated electron transfer to TiO₂ and successfully promoted synthesis of compounds. The use of a reusable photocatalyst without noble metal co-catalysts, along with the mild reaction conditions and use of light energy, make this method as an environmentally benign and energy saving chemical procedure.

Keywords: Heterogeneous catalysis, Photocatalysis; Titanium dioxide; Anatase/Rutile; Organic reactions; Nanoparticles

1. Introduction

Synthetic organic chemists pursuit towards novel reactions and chemo-selective transformations under green, mild and energy saving conditions are a continuous process [1-3]. Almost a century ago, in 1912, Giacomo Ciamician understood that light is a renewable and sustainable energy source for performing energy saving and green chemical reactions [4]. Since then, photochemistry has found wide utility in synthesis of organic compounds. But, the lack of light absorption *via* many organic compounds has limited the usage of photochemical synthesis. Therefore, employing light absorbing photocatalysts and employing their electron-energy transfer operations to produce organic compounds to accomplish required photochemical reactions would serve as an efficient tool for overcoming this barrier [5-8].

Among different types of semiconductors, titanium (IV) oxide is widely accepted as the best photocatalyst. TiO_2 has been broadly investigated lately as a potentially valuable material in the photocatalytic organic reactions due to its strong oxidizing ability, suitable band gap, high resistance to photo corrosion and chemical corrosion, low price and easy preparation [9-11]. But, the high recombination rate (about 90%) of photon induced electron-hole pairs reduces the photocatalytic efficiency of TiO_2 [12].

Previous reports have indicated that the physico-chemical factors of titanium dioxide materials, such as surface area, particle sizes and phase compositions, strongly influenced the photocatalytic efficiencies by restraining the charge recombination [13]. Especially, the crystallite phase dependent synergistic effect is often encountered in titanium dioxide photocatalysts, in which blended phases of rutile and anatase have been published to display higher efficiencies than their pure anatase compositions [14-18]. However, photocatalytic activity of pure TiO_2 especially in organic synthesis is low and its good performance is mainly achieved in the presence of noble metal co-catalysts, such as Pt, Pd, Au, etc [19-26]. To reduce the cost of organic synthesis, it is necessary to explore alternative co-catalysts based on

transition metals. Among them, Nickel oxide (NiO) as a *p*-type co-catalyst, with an indirect band gap of about 3.55 eV, is considered as the most effective choice because of its unique catalytic effect, low cost and so on Refs [27-30]. As above mentions, to improve the catalytic and photocatalytic efficiency, the *p*-type semiconductor NiO (hole-rich), can be coupled to an *n*-type semiconductor TiO₂ (electron-rich) which produce an *n*-*p* junction in the interface as a space charge region [31, 32]. This *n*-*p* junction along with mixing of anatase and rutile phases on TiO₂ occurs as an inner electric field by the equilibrium of electron and hole diffusion, which improves the catalytic and photocatalytic activity.

As part of our continuing efforts to develop green synthetic methods [33-35], herein we wish to report an energy saving and efficient protocol for the synthesis of benzimidazoles, imines and selective oxidation of alcohols at room temperature using NiO@anatase/rutile-TiO₂ as an efficient, cost-effective and reusable photocatalyst (Scheme 1).

2. Experimental

2.1. Materials

All the chemical reagents used in our experiments were purchased from Merck and Sigma-Aldrich and were used as received without further purification.

2.2. Preparation of NiO@anatase/rutile-TiO₂ and NiO@anatase-TiO₂ nanoparticles

NiO@Anatase/rutile-TiO₂ and NiO@anatase-TiO₂ NPs were prepared from a powder mixture of the corresponding component solid oxides, according to the following steps. First, 1 g of TiO₂ and NiO powders were grounded thoroughly in an agate mortar. Then the mixed oxides were dispersed in 100 mL boiling deionized water and sonicated for 5 min using a probe sonicator. After that the suspension solution was stirred for 24 h and then dried in an air oven at 80°C for 12 h. Finally, the dried solids were

calcined at different temperatures (see Fig. 2) for 1 h to prepare catalysts with anatase/rutile phases in different ratios.

2.3. Photocatalytic activity of NiO@anatase/rutile-TiO₂ in organic reactions

The photocatalytic reaction processes were carried out at room temperature in a batch quartz reactor. Artificial irradiation was provided by a 55W (UV-C) mercury lamp (Philips, Holland) emitting around 254 nm, positioned on top of the batch quartz reactor.

2.3.1. Selective oxidation of alcohols

The catalyst (3 mol%) was added to alcohol (5 mL) and dispersed by ultrasonication for 5 min. Then the suspension was added to a batch quartz reactor and photo-irradiated under magnetic stirring for appropriate times (see Table S1). After completion of reaction, the catalyst was recovered by centrifugation. The crude products were determined by ¹H-NMR and FT-IR.

2.3.2. Synthesis of benzimidazoles

The catalyst (3 mol%) was added to alcohol (5 mL) containing *ortho*-phenylenediamine (1 mmol) and dispersed by ultrasonication for 5 min. Then the suspension was added to a batch quartz reactor and photo-irradiated under magnetic stirring for appropriate times (see Table S2). After completion of reaction, the catalyst was recovered by centrifugation. The crude products were determined by ¹H-NMR, FT-IR and melting point.

2.3.3. Synthesis of Imines

The catalyst (3 mol%) was added to alcohol (5 mL) containing corresponding imine (1 mmol) and dispersed by ultrasonication for 5 min. Then the suspension was added to a batch quartz reactor and photo-irradiated under magnetic stirring for appropriate times (see Table S3). After completion the reaction, the catalyst was recovered by centrifugation. The organic solvent was removed under reduced

pressure to afford the respective imines. The crude products were determined by ^1H -NMR, FT-IR and melting point.

3. Results and discussion

3.1. Preparation and characterization of NiO@anatase/rutile-TiO₂ nanoparticle

NiO@anatase/rutile-TiO₂ nanoparticles were prepared from a powder mixture of the corresponding component solid oxides by using an impregnation method (Fig. S5) [28]. The synthesized materials were characterized by X-ray diffraction (XRD), high-resolution transmission electron microscopy (HRTEM), scanning electronic microscopy (SEM), energy dispersive X-ray spectroscopy (EDS) and Fourier transform infrared spectroscopy (FT-IR).

$$D = \frac{K\lambda}{\beta \cos\theta} \quad (1)$$

Where FWHM (full-width at half-maximum or half-width) is in radians and θ is the position of the maximum of diffraction peak, K is the so-called shape factor, which usually takes a value about 0.9, and λ is the X-ray wavelength. Crystallite size of NiO@anatase/rutile-TiO₂ nanoparticle has been found to be 42 nm.

Results in Fig. 2a show that changing the phase content of coupled sample critically depends on calcination temperature. As confirmed by X-ray diffraction analysis in Fig. 2b, with increasing of calcination temperature, rutile phase ratio increases and anatase phase ratio decreases, so that in the sample calcined at 550°C crystalline phase is anatase and in the sample calcined at 850°C major crystalline phase is rutile to be ~54%. The (101) reflection ($2\theta = 25.28^\circ$) of anatase, the (110) reflection ($2\theta = 27.42^\circ$) of rutile and the (200) reflection ($2\theta = 43.31^\circ$) of NiO were used for comparisons.

The phase content of prepared nanoparticles was calculated by the following equation, where, I_A is integrated intensity of the anatase (101) diffraction peak and I_R is integrated intensity of the rutile (110) diffraction peak.³⁴

$$\text{Anatase phase}\% = \frac{100}{1+0.8(I_A/I_R)} \quad (2)$$

HRTEM image of the NiO@anatase/rutile-TiO₂ nanoparticles calcined at 650 °C (contain 87:13 anatase:rutile ratio) with 30 wt% content of NiO are shown in Fig. 3a. The average particle size of the TiO₂ nanoparticles in mixed phases system is assessed to be approximately 50 nm, which is in compromise with the average crystallite size determined from the XRD patterns. Furthermore, the small NiO particles with average diameter of 10 nm were observed on the surface of TiO₂ particles by the HRTEM image.

The DRS spectra of pure NiO, pure TiO₂, and optimized 30%NiO@anatase/rutile-TiO₂ nanoparticles are illustrated in Fig. S1 (Supporting Information). The values of band gap energy, via analogizing the linear part of the spectra and determining its intersection with energy axis, were determined to be 3.55, 3.28, and 3.31 eV, respectively. The attained results specified that with NiO coupling, the band gap energy of pristine TiO₂ increases by 0.05 eV, displaying a blue shift. So, the electron hole separation time is comparatively longer in the NiO@anatase/rutile-TiO₂ than pure TiO₂.

The Raman spectra of 30%NiO@anatase/rutile-TiO₂ is shown in Fig. S9 (Supporting Information). The Raman peaks located at 198, 394, 514, 634 cm⁻¹ correspond to the anatase phase and the peaks located at 240, 443, 610 cm⁻¹ correspond to the rutile phase of TiO₂. Moreover, the broad peak observed at 508 cm⁻¹ corresponds to NiO [36, 37].

3.2. Photocatalytic activity of NiO@TiO₂ nanoparticle in organic reactions

In order to investigate the effects of this nano photocatalyst, catalytic and photocatalytic performance of NiO@TiO₂ were considered in the different organic reactions including synthesis of benzimidazoles, synthesis of imines and selective oxidation of alcohols. In these reactions ethanol, aniline and *ortho*-phenylenediamine were used as initial material for model reactions. To optimize the synthesis conditions the NiO content of photocatalyst and ratio of anatase:rutile phases of TiO₂ were investigated in dark and light conditions.

Firstly to evaluate the effect of the NiO quantity on the catalytic and photocatalytic activity of NiO@anatase/rutile-TiO₂ NPs, Various contents of NiO were used in the preparation process. As shown in Fig. S6 the product yields in all of the reactions were increased with the NiO weight ratio to 30 wt % in coupled nanoparticles. Also the result of Fig. S7 is shown the optimum amount of the catalyst was (3 mol%) of NiO@anatase/rutile-TiO₂ NPs which increasing of this amount did not show any significant change in yield of reactions.

Subsequently, for comparison of photocatalytic activity in NiO@anatase-TiO₂ and NiO@anatase/rutile-TiO₂, the reactions in the dark and light at room temperature are provided in Table 1. Also, control experiments using pure anatase TiO₂ as the catalyst was performed.

The results in table 1 show an interesting trend. For all reactions conducted in the dark, the NiO@anatase/rutile-TiO₂, NiO@anatase-TiO₂ and pure anatase TiO₂ didn't exhibit substantial activity. Moreover, the obtained results were indicated that in absence of catalyst, trace amounts of products were generated. But the NiO@anatase/rutile-TiO₂ NPs exhibited superior photocatalytic activity to both the NiO@anatase-TiO₂ and the pure anatase TiO₂ NPs in the presence of light irradiations. As can be seen in Table 1, the NiO@anatase/rutile-TiO₂ NPs increased the product yield of the benzimidazoles to 98% (from 80% using NiO@anatase-TiO₂), and the yield of imines to 99% (from 81% using NiO@anatase-TiO₂), and the yield of benzyl alcohols to >99% (from 84% using NiO@anatase-TiO₂).

Finally, to achieve NiO@TiO₂ photocatalyst with high catalytic and photocatalytic activity, we have screened the effect of the rutile and anatase phases ratio in the catalytic and photocatalytic activity of the NiO@anatase/rutile-TiO₂ NPs in model reactions. Results in figure S8 show that an anatase/rutile ratio of TiO₂ with 87:13 ratio is the best choice for these reactions.

Therefore, the study was extended to prepare benzimidazoles, imines and selective oxidation of benzyl alcohol using anatase/rutile-TiO₂@30%NiO NPs with 87:13 of anatase/rutile ratio. The detailed data of these three reactions are provided in Tables S1-S3.

The results in Tables S1-S3 show that, NiO@anatase/rutile-TiO₂ under UV light irradiation at room temperature is the suitable catalyst for maximizing the yield of these reactions. This catalyst promoted selective oxidation of alcohols and synthesis of benzimidazoles and imines in high yields and the yields were higher than those of obtained NiO@anatase-TiO₂ under UV at room temperature.

The reasons of the excellent photocatalytic activity of NiO@anatase/rutile-TiO₂ NPs may be the phenomenon of p-n junction formed between NiO and TiO₂ as well as difference between band gaps in rutile and anatase phases. When NiO as a p-type hole-rich semiconductor is in contact with TiO₂ as an n-type electron-rich semiconductor, at p-n junction interfacial contact produces a space charge region. In n-p junction interfacial contact the holes are diffused from TiO₂ to NiO and electrons are diffused from NiO to TiO₂. On the other hands, the phase junction between anatase and rutile provides a synergistic effect, easing effective electron-hole separation. As previous reports [14,38], a band alignment of about 0.4 eV exists between rutile and anatase (with rutile possessing a lower electron affinity) enabling photo-generated CB electrons flow from rutile phase to anatase phase. As result, a strong separation of electron-hole pairs between the two phases as well as n-p junction between TiO₂ and NiO improvement of the photocatalytic activity.

3.3. Mechanism of Photocatalytic activity of the NiO@anatase/rutile-TiO₂ in organic reactions

On the basis of the cases described above, the mechanism for these reactions on the NiO@anatase/rutile-TiO₂ photocatalytic is described by the following mechanism, as summarized in Fig. 4 and scheme 2 [15,16,39]. As shown in Fig. 4 the electron injection from NiO nanoparticles to rutile accumulates electron in its conduction band and results in the negative shift of E_{CB}. This promotes the continuous electron transfer from the NiO particles to rutile and then to anatase and efficient O₂ reduction on the anatase surface. Therefore, the NiO@anatase/rutile joint active site promotes the reactions.

Mechanism of reactions at the joint active site is explained as in Scheme 2. (a) p-n junction of NiO particles transfers electrons to the tightly bound rutile; then the electron is moved to well-conjugated anatase; and O₂ is reduced thereby electron (formation of O–O– species). (b) The O–O– species probably attracts the H atom of the alcohol while the empty orbital on NiO adsorbs the lone pair of oxygen in alcohol (c). Subsequent removal of the H atom from this species produces the aldehydes **1**.

In the next step, the produced aldehydes **1** are activating by the Lewis acidity of NiO coupled with TiO₂ and then condensation with *ortho*-phenylenediamine **2** or imines **3** takes place to afford corresponding benzimidazoles **4** or imines **5**.

3.4. Recyclability Study of NiO@anatase/rutile-TiO₂ photocatalyst

The activity and stability of the catalyst was assessed by reusing and recycling experiments for the synthesis of benzimidazoles, imines and selective oxidation of alcohols under optimized reaction conditions and the results are shown in Fig. 5. After the experiment, the NiO@TiO₂ photocatalyst was separated from the reaction mixture by centrifugation, and washed with hot ethanol for three times to remove adsorbed organic impurities from its surface. The recovered photocatalyst was dried at 100 °C for 3 h and reused for the next runs under optimized reaction conditions. It was found that the NiO@anatase/rutile-TiO₂ photocatalyst could be recycled and reused for six times without significant loss in its photocatalytic and catalytic activity and its selectivity, as depicted in Fig. 5.

4. Conclusions

In this study tandem photocatalytic and catalytic activity of NiO@anatase/rutile-TiO₂ nanoparticles were investigated for the synthesis of some organic compounds including aldehydes, benzimidazoles and imines under UV-light irradiation. The photocatalytic activity strongly depends on the loadings of NiO on the TiO₂ (the amount of NiO was optimized to be 30 wt%) and the content of anatase/rutile phases in TiO₂ (the optimized content of anatase:rutile phases was 87%:13%). The significant advantages of this photocatalytic process over the previous reported processes for these organic reactions are: [18-24] (i) noble-metal free and inexpensive heterogeneous catalyst (NiO@TiO₂), (ii) reusable and recyclable catalyst (six times), (iii) safe and inexpensive reducing agent (alcohol), (iv) wide ranges of substrates (benzylic and aliphatic alcohols) and (v) mild reaction conditions (room temperature and atmospheric pressure). This method therefore, may help open a new strategy toward the design of more effective photocatalysts and the creation of new methods for photocatalysis based green organic synthesis.

Acknowledgments

The authors thank University of Tehran for the support of this work.

Appendix A. Supplementary data

Supplementary data associated with this article can be found in the online version.

References

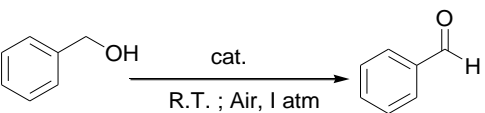
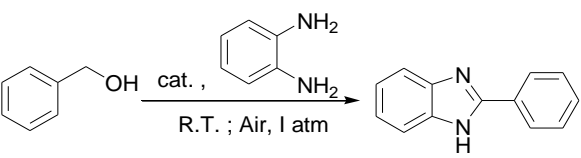
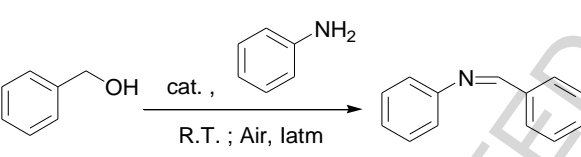
1. R. A. Sheldon, Chem. Soc. Rev. 41 (2012) 1437-1451.
2. J. C. Colmenares, R. Luque, Chem. Soc. Rev. 43 (2014) 765-778.
3. P. Anastas, N. Eghbali, Chem. Soc. Rev. 39 (2010) 301-312.

4. G. Ciamician, *Science* 36 (1912) 385-394.
5. X. Lang, X. Chen, J. Zhao, *Chem. Soc. Rev.* 43 (2014) 473-486.
6. T. P. Yoon, M. A. Ischay, J. Du, *Nature Chem.* 2 (2010) 527-532.
7. C. K. Prier, D. A. Rankic, D. W. MacMillan, *Chem. Rev.* 113 (2013) 5322-5363.
8. S. Sarina, H. Zhu, E. Jaatinen, Q. Xiao, H. Liu, J. Jia, J. Zhao, *J. Am. Chem. Soc.* 135 (2013) 5793-5801.
9. A. Fujishima, K. Hashimoto, T. Watanabe, BKC Incorporated; (1999).
10. A. L. Linsebigler, G. Lu, J. T. Yates Jr, *Chem. Rev.* 95 (1995) 735-758.
11. K. Hashimoto, H. Irie, A. Fujishima, *Jpn. J. Appl. Phys.* 44 (2005) 8269-8285.
12. X. Chen, S. S. Mao, *Chem. Rev.* 107 (2007) 2891-2959.
13. J. Schneider, M. Matsuoka, M. Takeuchi, J. Zhang, Y. Horiuchi, M. Anpo, D. W. Bahnemann, *Chem. Rev.* 114 (2014) 9919-9986.
14. D. O. Scanlon, C. W. Dunnill, J. Buckeridge, S. A. Shevlin, A. J. Logsdail, S. M. Woodley, A. A. Sokol, *Nat. Mater.* 12 (2013) 798-801.
15. Y. Shiraishi, H. Sakamoto, K. Fujiwara, S. Ichikawa, T. Hirai, *ACS Catal.* 4 (2014) 2418-2425.
16. H. Li, W. Zhang, W. Pan, *J. Am. Ceram. Soc.* 94 (2011) 3184-3187.
17. T. Kawahara, Y. Konishi, H. Tada, N. Tohge, J. Nishii, S. Ito, *Angew. Chem.* 114 (2002) 2935-2937.
18. H. Hirakawa, M. Katayama, Y. Shiraishi, H. Sakamoto, K. Wang, B. Ohtani, S. Ichikawa, S. Tanaka, T. Hirai, *ACS Appl. Mater. Interfaces* 7 (2015) 3797-3806.
19. Y. Shiraishi, Y. Sugano, S. Tanaka, T. Hirai, *Angew. Chem. Int. Ed.* 49 (2010) 1656-1660.
20. K. Selvam, B. Krishnakumar, R. Velmurugan, M. A. Swaminathan, *Catal. Commun.* 11 (2009) 280-284.

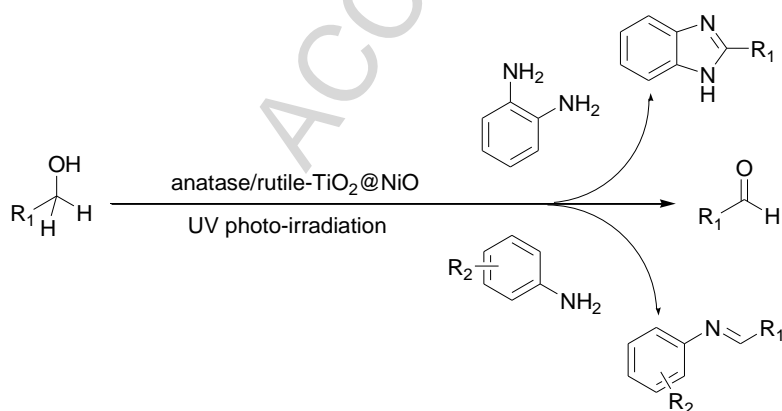
21. Y. Shiraishi, K. Fujiwara, Y. Sugano, S. Ichikawa, T. Hirai, *ACS Catal.* 3 (2013) 312-320.
22. D. Stíbal, J. Sá, J. van Bokhoven, *Catal. Sci. Technol.* 3 (2013) 94-98.
23. D. Tsukamoto, Y. Shiraishi, Y. Sugano, S. Ichikawa, S. Tanaka, T. Hirai, *J. Am. Chem. Soc.* 134 (2012) 6309-6315.
24. Y. Shiraishi, M. Ikeda, D. Tsukamoto, S. Tanaka, T. Hirai, *Chem. Commun.* 47 (2011) 4811-4813.
25. J. Zhao, Z. Zheng, S. Bottle, A. Chou, S. Sarina, H. Zhu, *Chem. Commun.* 49 (2013) 2676-2678.
26. T. Kamegawa, H. Seto, S. Matsuura, H. Yamashita, *ACS Appl. Mater. Interfaces* 4 (2012) 6635-6639.
27. S. H. Choi, J. H. Lee, Y. C. Kang, *Nanoscale* 5 (2013) 12645-12650.
28. K. Chockalingam, A. Ganapathy, G. Paramasivan, M. Govindasamy, A. Viswanathan, *J. Am. Ceram. Soc.* 94 (2011) 2499-2505.
29. H. Eskandarloo, A. Badiei, M. A. Behnajady, *Ind. Eng. Chem. Res.* 53 (2014) 6881-6895.
30. C. J. Chen, C. H. Liao, K. C. Hsu, Y. T. Wu, J. C. Wu, *Catal. Commun.* 12 (2011) 1307-1310.
31. Q. Jin, T. Ikeda, M. Fujishima, H. Tada, *Chem. Commun.* 47 (2011) 8814-8816.
32. A. Iwaszuk, M. Nolan, Q. Jin, M. Fujishima, H. Tada, *J. Phys. Chem. C* 117 (2013) 2709-2718.
33. A. Ziarati, J. Safaei-Ghomi, S. Rohani, *Ultrason. Sonochem.* 20 (2013) 1069-1075.
34. J. Poostforooshan, A. Badiei, M. Kolahdouz, A. P. Weber, *ACS Appl. Mater. Interfaces* 8 (2016) 21731-21741.
35. H. Eskandarloo, M. Hashempour, A. Vincenzo, S. Franz, A. Badiei, M. A. Behnajady, M. Bestetti, *Appl. Catal., B.* 185 (2016) 119-132.
36. O. Frank, M. Zukalova, B. Laskova, J. Kurti, J. Koltai, L. Kavan, *Phys. Chem. Chem. Phys.* 14 (2012) 14567-14572.

37. D. C. Joshi, S. Nayak, A. Kumar, A. Mohanta, D. Pamu, S. Thota, J. Appl. Phys. 119 (2016) 74303-73310.
38. R. A. Spurr, H. Myers, Anal. Chem. 29 (1957) 760-762.
39. Z. Xiong, H. Wu, L. Zhang, Y. Gu, X. S. Zhao, J. Mater. Chem. A 2 (2014) 9291-9297.

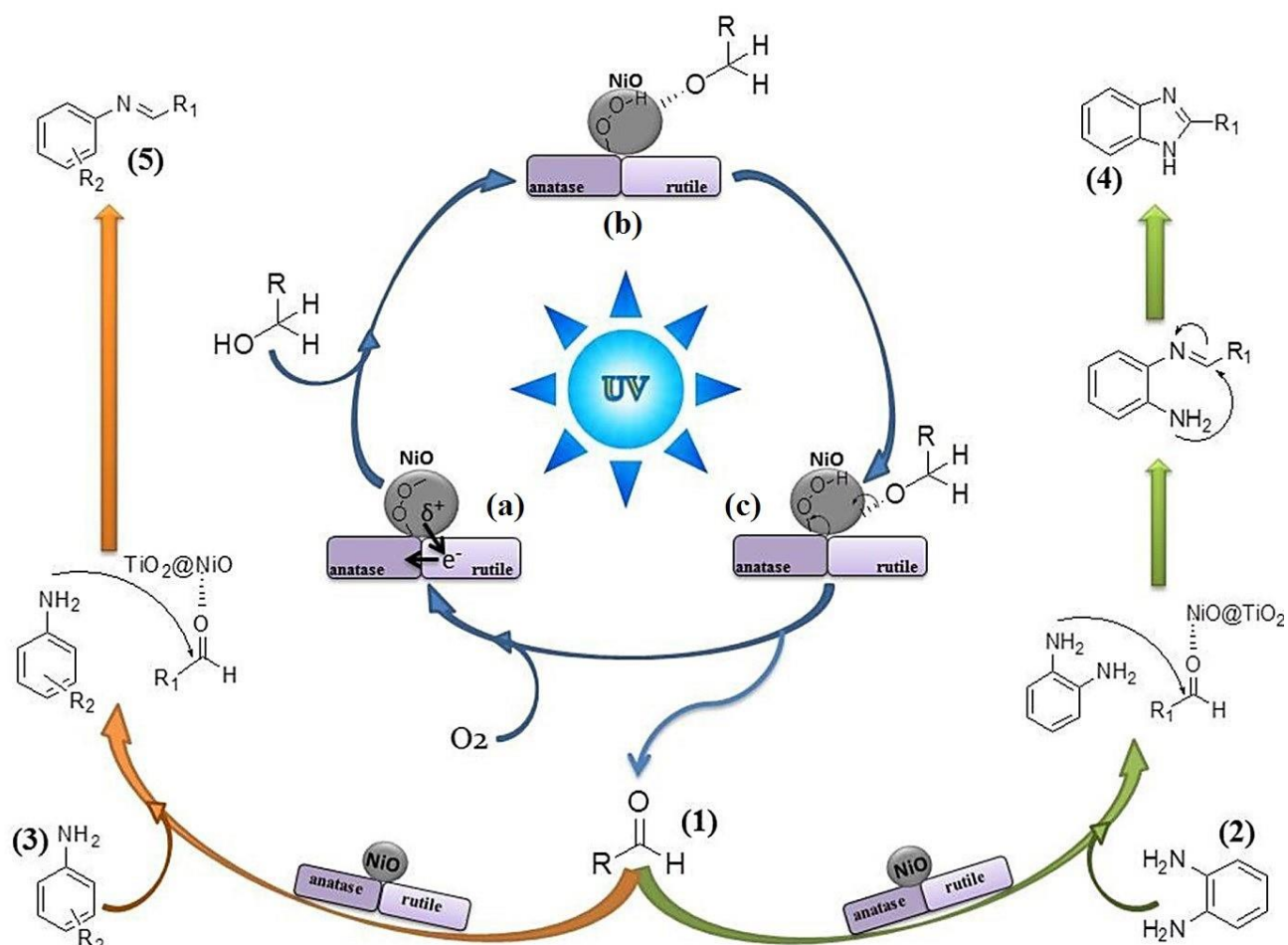
Table 1. Comparison of the photocatalytic activity in organic reactions

Reaction	Light ^a	Yield of reactions (%)			
		Without catalyst	TiO ₂	NiO@anatase -TiO ₂	NiO@anatase / rutile-TiO ₂
1) Selective oxidation of alcohol	UV	trace	48	83	>99
	Dark	0	21	25	26
2) Synthesis of benzimidazole	UV	trace	31	80	98
	Dark	0	14	22	23
3) Preparation of imine	UV	trace	34	81	99
	Dark	0	17	23	25

^aThe data of the reactions in the dark are provided for comparison



Scheme 1. Photocatalytic and catalytic activity of the NiO@anatase/rutile-TiO₂ in organic reactions



Scheme 2. Proposed mechanism for the synthesis of benzimidazole, imines and aldehydes promoted by an NiO@anatase/rutile-TiO₂ under photo-irradiation

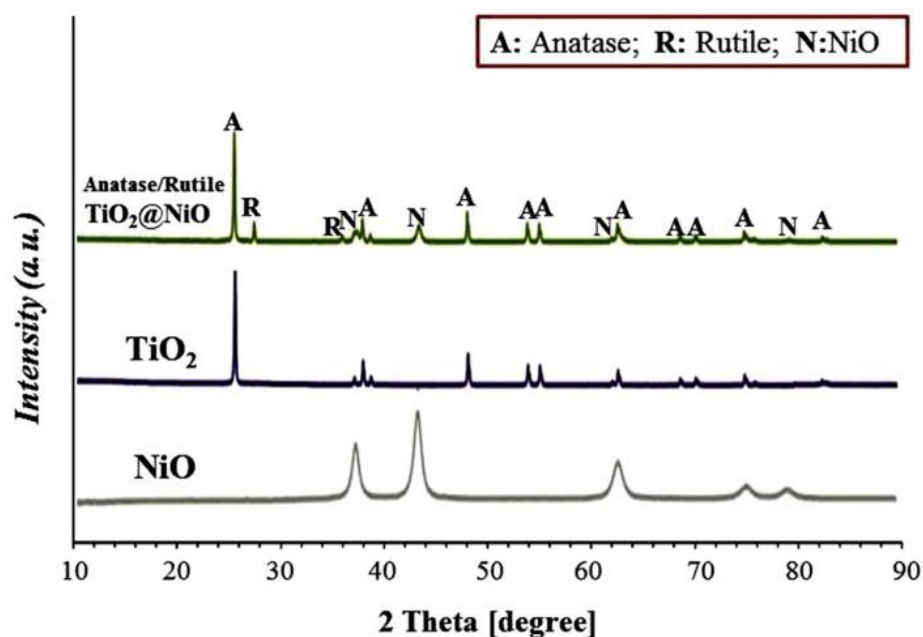


Fig. 1. XRD patterns of TiO_2 , NiO and $\text{NiO@anatase/rutile-TiO}_2$ nanoparticles

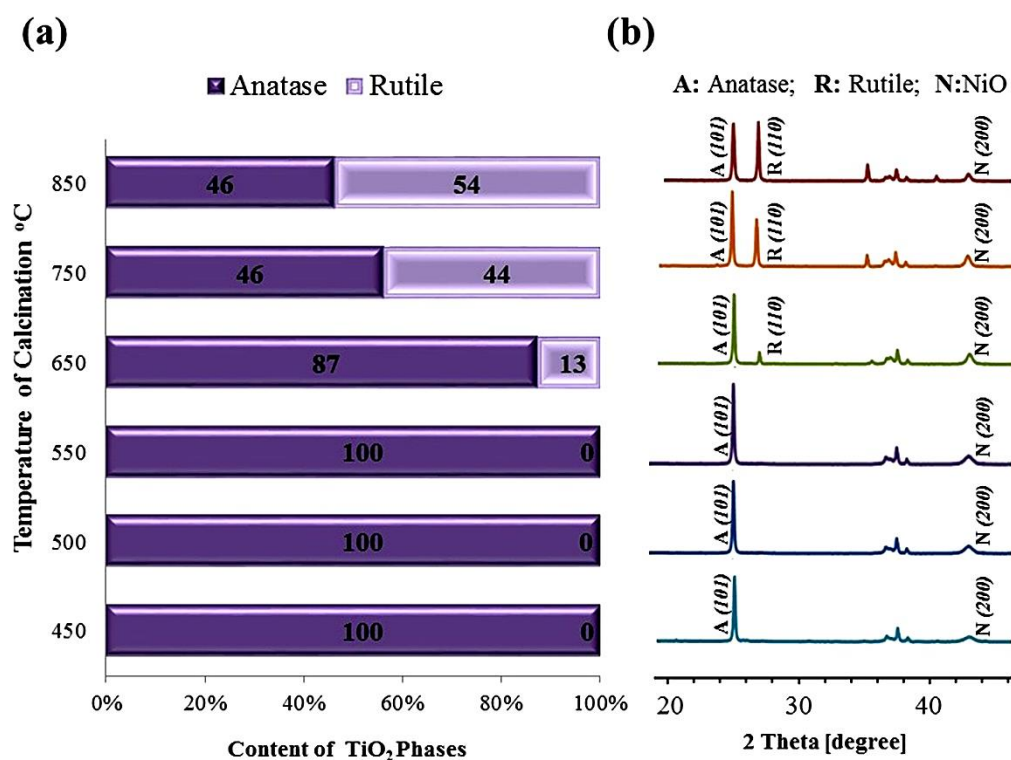


Fig. 2. Anatase and rutile phase content of NiO@TiO_2 in different calcination temperature

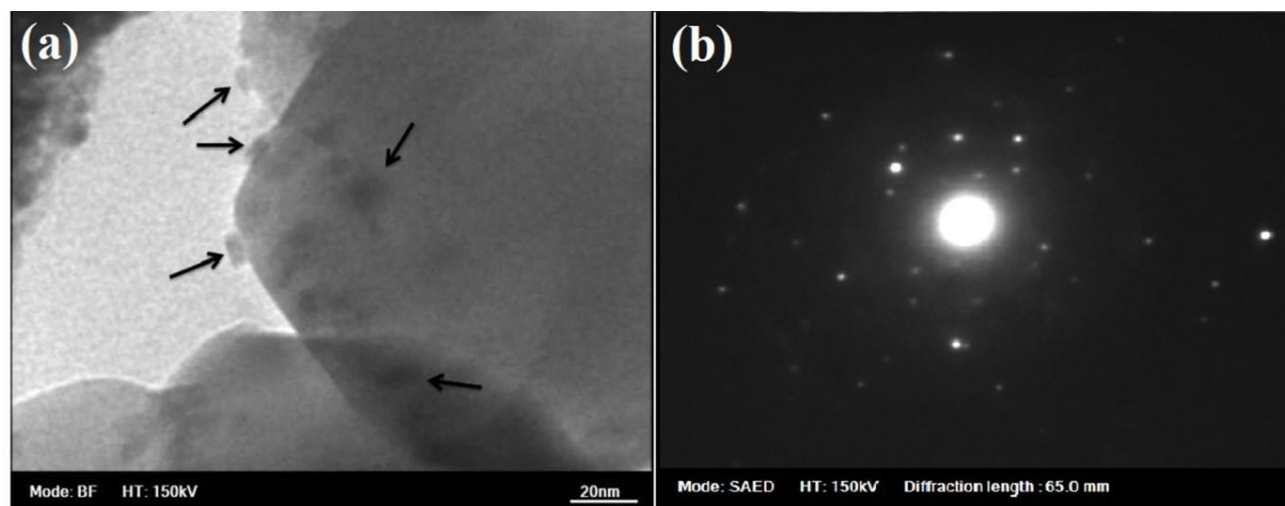


Fig. 3. (a) HRTEM image of the NiO@anatase/rutile-TiO₂ (the arrows indicate NiO nanoparticles); (b) SAED pattern of the NiO@anatase/rutile-TiO₂ nanoparticles

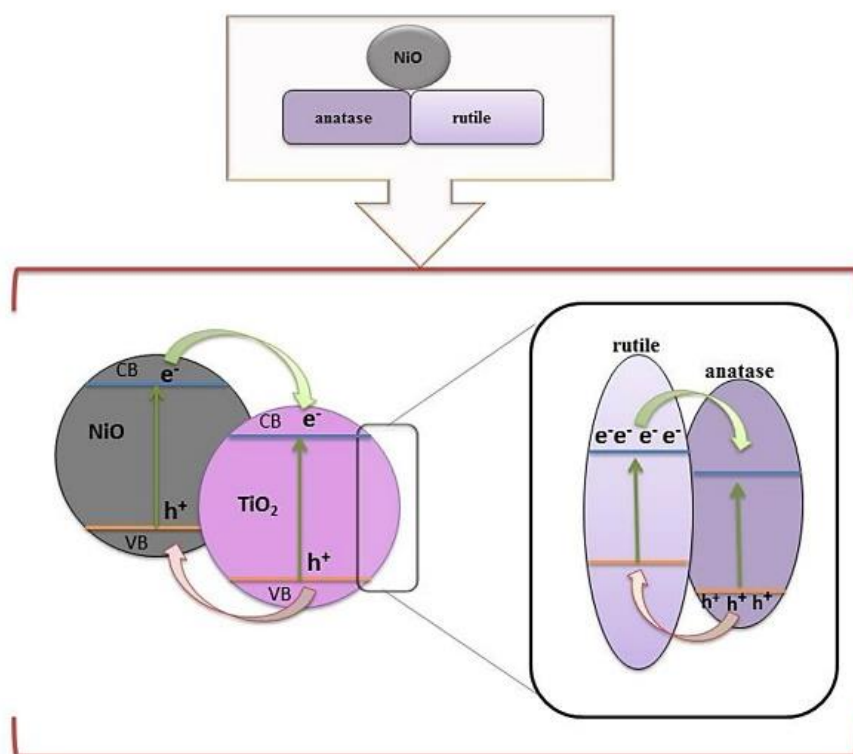


Fig. 4. Schematic of the valence and conduction band alignment mechanism for anatase–rutile interface coupled by NiO

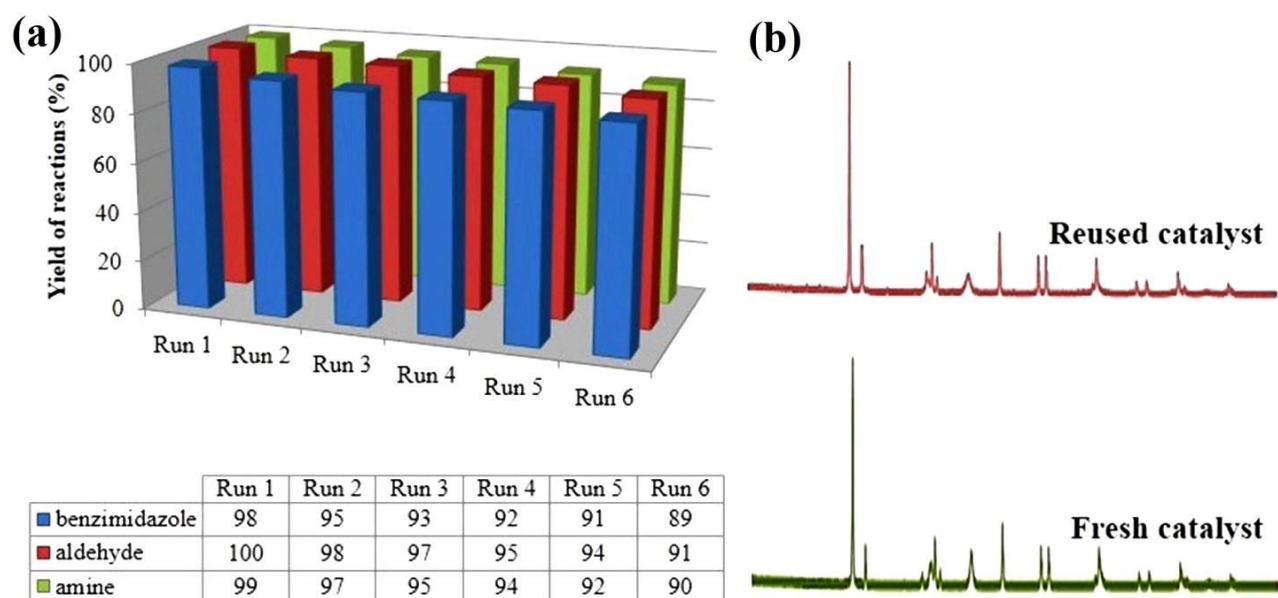
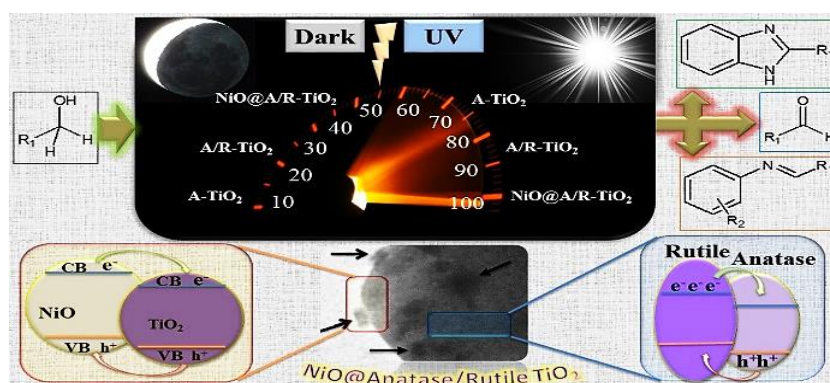


Fig. 5. (a) Reuseability Study of NiO@anatase/rutile-TiO₂ photocatalyst in organic reactions. (b) XRD patterns of photocatalyst before used and after six times reused.

Graphical Abstract



A noble-metal free reusable NiO@anatase/rutile-TiO₂ nanoparticles photocatalyzed selective synthesis of organic compounds under UV-irradiation at room temperature

Highlights

- NiO coupled with anatase/rutile phases of TiO₂ were prepared by impregnation route
- The p-n junction NiO@anatase/rutile-TiO₂ was employed as efficient photocatalyst
- This nanostructure exhibited superior photocatalytic activity in organic reactions
- 30%NiO coupled with 87:13 of anatase:rutile phases ratio showed highest activity
- The activity of this nanocatalyst was nearly the same after six times of recycling